PHYSICAL REVIEW C **80**, 051303(R) (2009)

Microscopic calculation of α-decay half-lives with a deformed potential

Dongdong Ni[1,3,*] and Zhongzhou Ren[1,2,3,†]

[1]*Department of Physics, Nanjing University, Nanjing 210093, People's Republic of China*

[2]*Center of Theoretical Nuclear Physics, National Laboratory of Heavy-Ion Accelerator, Lanzhou 730000, People's Republic of China*

[3]*Kavli Institute for Theoretical Physics China, Beijing 100190, People's Republic of China*

(Received 23 July 2009; revised manuscript received 11 October 2009; published 12 November 2009)

A new version of the generalized density-dependent cluster model is presented to describe an α particle tunneling through a deformed potential barrier. The microscopic deformed potential is numerically constructed in the double-folding model by the multipole expansion method. The decay width is computed using the coupled-channel Schrödinger equation with outgoing wave boundary conditions. We perform a systematic calculation on α-decay half-lives of even-even nuclei ranging from $Z = 52$ to $Z = 104$, including 65 well-deformed ones. The calculated α-decay half-lives are found to be in good agreement with the experimental values. There also exists good agreement with the available experimental branching ratios for well-deformed systems.

DOI: 10.1103/PhysRevC.80.051303 PACS number(s): 23.60.+e, 21.10.Tg, 21.60.Gx

Alpha decay was described in 1928 as a quantum mechanical tunneling effect [1,2]. The decay process can be divided into two distinct parts: the formation of an α particle at the nuclear surface, followed by its tunneling through the α-daughter potential barrier. To compute the α-formation amplitude various approaches have been developed, such as the shell model including Bardeen-Cooper-Schriefer (BCS) pairing [3], the hybrid model supplementing the shell-model wave function with an α-cluster component [4], and even the way of extracting the preformation factor from the experimental half-lives [5]. Whatever the formation mechanism, the decay proceeds by a quantum tunneling through the potential barrier. If this barrier is assumed to be spherical, the theoretical evaluation of the decay width is a simple task no matter whether it concerns the Wentzel-Kramers-Brillouin (WKB) semiclassical approximation or the exact quantum mechanics description [6–10]. Actually, various calculations with different potentials are usually performed with this assumption of spherical shapes, because in most cases the ground states of α emitters are spherical or moderately deformed. All of them should be considered as an effective theory for α decay [11–17]. Despite these theoretical achievements, the actual situation of α decay is much more complicated than what we expect. The observation of fine structure in α decay has often been attributed to the tunneling of the α particle through a deformed barrier [18,19]. A complete explanation of the α-decay process should be able to describe the effect of core deformation.

Recently we have studied exotic α decays around the $N = 126$ shell gap within the spherical version of the generalized density-dependent cluster model (GDDCM) [20]. In this case, where the decaying nucleus is regarded as a core nucleus plus an α cluster moving in a spherical potential, one only needs to solve a single radial equation for the exact quantum mechanics value of the decay width [21–24]. This work is an extension of the model toward a deformed case, where the parent nucleus is described by an α particle moving in a deformed potential. On the one hand, the deformed potential is numerically constructed in the well-established double-folding model by the multipole expansion method [25,26]. On the other hand, of course the violation of spherical symmetry leads to the coupled-channel effect between outgoing waves with $\ell = 0, 2$. Note that $\ell \geqslant 4$ α transitions are strongly restrained by the centrifugal barrier. Therefore, it is necessary to perform a full coupled-channel calculation for deformed systems.

Consider a deformed system formed by an axial-symmetric core nucleus with quadrupole and hexadecapole deformations plus a spherical α cluster. The wave function of a single α cluster in a quasibound state can be expanded into a sum of partial waves with angular and radial components [19,27,28],

$$\Psi(\mathbf{r}, \Omega_d) = \frac{1}{r}\sum_{\alpha} u_\alpha(r)\Theta_\alpha(\Omega, \Omega_d), \tag{1}$$

where $\alpha \equiv (n\ell j)$ completely denotes the channel quantum number, the angular part is written as $\Theta_\alpha(\Omega, \Omega_d) = [Y_\alpha(\Omega) \otimes Y_\alpha(\Omega_d)]_{00}$. Inserting Eq. (1) into the Schrödinger equation and projecting it onto the channel states, one obtains the usual coupled-channel equations for radial components [19,27,28],

$$\left\{-\frac{\hbar^2}{2\mu}\left[\frac{d^2}{dr^2} - \frac{\ell_\alpha(\ell_\alpha+1)}{r^2}\right] - Q_{J_d}\right\} u_\alpha(r) + \sum_{\alpha'} V_{\alpha,\alpha'}(r)u_{\alpha'}(r) = 0, \tag{2}$$

where μ is the reduced mass of the system and Q_{J_d} is the energy of the emitted α particle leaving the daughter nucleus in the state J_d. The interaction matrix that contains all of nuclear physics is given by

$$V_{\alpha,\alpha'}(r) = (\Theta_\alpha(\Omega, \Omega_d)||V(\mathbf{r}, \Omega_d)||\Theta_{\alpha'}(\Omega, \Omega_d)), \tag{3}$$

where the parentheses denote integration over all coordinates, save the radial variable r.

The interaction between the center of mass of the core and the α cluster is obtained using the double-folding integral of the realistic nucleon-nucleon (NN) interaction with the density distributions of the α particle and the core nucleus [25,26,29];

*dongdongnick@gmail.com
†zren@nju.edu.cn

that is,

$$V(\mathbf{r}, \Omega_d) = \lambda \int d\mathbf{r_1} d\mathbf{r_2} \rho_1(\mathbf{r_1}) \upsilon(\mathbf{s}) \rho_2(\mathbf{r_2}), \tag{4}$$

where λ is the renormalized factor and $\upsilon(\mathbf{s} = |\mathbf{r} + \mathbf{r_2} - \mathbf{r_1})$ is the effective NN interaction. The spherical density distribution of the α particle $\rho_1(\mathbf{r_1})$ is taken as a standard Gaussian form [15]. The deformed density distribution of the core nucleus $\rho_2(\mathbf{r_2})$ has the form

$$\rho_2(r_2, \theta) = \frac{\rho_0}{1 + e^{[r - R(\theta)]/a}}, \tag{5}$$

where the half-density radius $R(\theta)$ is parametrized as $R(\theta) = R_0[1 + \beta_2 Y_{20}(\theta) + \beta_4 Y_{40}(\theta)]$.

In view of the deformed density distribution in the six-dimensional integral, it is a difficult undertaking to derive the microscopic α-nucleus potential. In this case, one usually simplifies the double-folding model by expanding the density distribution of the deformed nuclei using a multipole expansion [25]. The density distribution of the axial-symmetric daughter nucleus is expanded as [25,26]

$$\rho_2(r_2, \theta) = \sum_{\ell = \text{even}} \rho_2^{\ell}(r_2) Y_{\ell 0}(\Omega_d). \tag{6}$$

The sum is usually truncated at $\ell = 4$. Then the double folding potential can be evaluated as the sum of different multipole components [25,26],

$$\begin{aligned} V(\mathbf{r}, \Omega_d) &= \sum_{\ell = 0,2,4\ldots} V^{\ell}(r) \Theta_{\ell}(\Omega, \Omega_d) \\ &= \sum_{\ell = 0,2,4\ldots} \frac{2}{\pi} \int_0^{\infty} dk k^2 j_{\ell}(kr) \tilde{\rho}_1(k) \\ &\quad \times \tilde{\rho}_2^{\ell}(k) \tilde{v}(k) \Theta_{\ell}(\Omega, \Omega_d), \end{aligned} \tag{7}$$

where $\tilde{\rho}_1(k)$ is the Fourier transformation of the density distribution of the α particle, $\tilde{\rho}_2^{\ell}(k)$ is the intrinsic form factor corresponding to the daughter nucleus, and $\tilde{v}(k)$ is the Fourier transformation of the effective M3Y NN interaction [30,31]. As the interaction is expressed in multipoles, the manipulation of the interaction matrix presents no further problem. The matrix elements can then be written in terms of the Clebsch-Gordan coefficient as follows:

$$\begin{aligned} V_{\alpha,\alpha'}(r) &= \sum_{\ell = 0,2,4\ldots} V^{\ell}(r) \sqrt{\frac{(2\ell + 1)(2\alpha + 1)}{4\pi(2\alpha' + 1)}} \\ &\quad \times (\langle \alpha, 0, \ell, 0 | \alpha', 0 \rangle)^2. \end{aligned} \tag{8}$$

At a large distance R the nuclear potential vanishes and the Coulomb potential is spherically symmetric. At this point the coupled-channel equations decouple. Therefore the wave functions of Eq. (2) at R behave as in the spherical case [23,24,32]:

$$u_{n\ell j}(r) = N_{\ell j} G_{\ell}(k_{J_d} r), \tag{9}$$

where $N_{\ell j}$ are normalization constants and $G_{\ell}(k_{J_d} r)$ is the irregular Coulomb wave function with $k_{J_d} = \sqrt{2\mu Q_{J_d}}/\hbar$. We know that the strict matching condition requires a complex wave function, $O_{\ell}(k_{J_d} r) = G_{\ell}(k_{J_d} r) + i F_{\ell}(k_{J_d} r)$. However, considering that the α-decay width associated with the imaginary part is usually extremely small, one could as well use the real wave function $G_{\ell}(k_{J_d} r)$ instead, as shown by Refs. [23,24,32]. As usual, one can express the partial width of the channel ℓj in terms of the normalization constant,

$$\Gamma_{\ell j}(R) = \frac{\hbar^2 k_{J_d}}{\mu} |N_{\ell j}|^2 = \frac{\hbar^2 k_{J_d}}{\mu} \frac{|u_{n\ell j}(R)|^2}{|G_{\ell}(k_{J_d} R)|^2}. \tag{10}$$

It is worth pointing out that Eq. (10) is valid only for distances outside the range of the nuclear potential and independent of R.

Because the decay energy cannot be predicted with sufficient accuracy for a given potential, as before, we adjust the renormalized factor λ to make all channels simultaneously characterized by the experimental Q_{J_d}. This means that the α-nucleus potential remains the same for all channels of a given α emitter. Then, to account for the Pauli exclusion principle, the quantum number n (i.e., the number of internal nodes) is chosen by the Wildermuth condition [12–15,33],

$$G = 2n + \ell = \sum_{i=1}^{4} g_i. \tag{11}$$

In this expression, g_i are the corresponding oscillator quantum numbers of the nucleons composing the cluster, whose values are restricted by the Pauli principle. In addition, the M3Y NN interaction used in the double-folding model includes a zero-range potential for the single-nucleon exchange. This term guarantees the antisymmetrization of identical nucleons in the α cluster and in the core nucleus [29–31].

The total width representing the tunneling through the deformed barrier is a sum of partial channel widths,

$$\Gamma(R) = \sum_{\{\ell j\}} \Gamma_{\ell j}(R), \tag{12}$$

where $\Gamma_{\ell j}(R)$ corresponding to the decay into a core state J_d is given by Eq. (10). Furthermore, it is convenient to perform a straightforward calculation of branching ratios within this framework. The branching ratio for α transitions to a core state J_d is written as

$$b_{J_d}\% = \Gamma_{\ell j}(R)/\Gamma(R) \times 100\%. \tag{13}$$

In all of these derivations it is assumed that the deformation of the daughter nucleus remains the same as in the decaying nucleus.

In the spherical case, the radius and the diffuseness of the density distribution of the core nucleus are taken as $R_0 = 1.07$ fm and $a = 0.50$ fm; this parametrization turns out to work very well in the description of spherical α emitters [20,24]. As a further extension toward deformed systems, we assume that the α-nucleus potential should be the same for the core nucleus in its ground or excited state so that it is not necessary to introduce other new parameters, which would reduce the predictive power of the calculation. Unfortunately, it is found that the above parameter set has too small a radius to give a quantitative description of the tunneling rate. This is very similar to the situation of proton emission, where the Becchetti-Greenlees Woods-Saxon parameter set is excellent for spherical proton emitters but performs rather poorly for deformed ones for the same reason [23,28]. With this in mind,

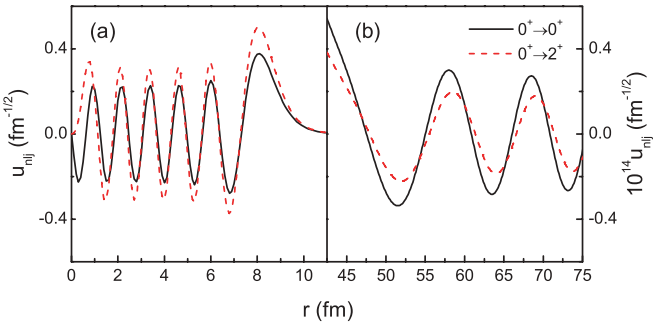

FIG. 1. (Color online) Schematic plot of two-channel wave functions in the α decay of the nucleus ^{242}Cm. The solid line (black) and the dash line (red), respectively, denote the $0^+ \to 0^+$ and $0^+ \to 2^+$ channel functions, with the same renormalized factor $\lambda = 0.711$. Note that the y axis in panel (b) is magnified by 10^{14}.

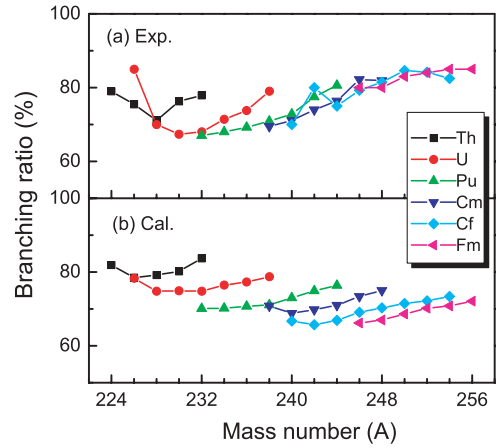

FIG. 2. (Color online) Comparison of the calculated branching ratios for $0^+_{\text{g.s.}} \to 0^+_{\text{g.s.}}$ α transitions with the available experimental data.

as in the case of proton emission, a new parameter set, which has slightly larger radii, is taken for deformed α emitters as follows: $R_0 = 1.15$ fm and $a = 0.50$ fm.

As the last step toward calculating α-decay half-lives, we need knowledge of the preformation factor P_α. It can be evaluated, in principle, from the overlap between the actual wave function of the parent nucleus and the decaying state wave function describing one α cluster coupled to the residual core nucleus. However, it is extremely difficult to obtain the actual wave functions mentioned previously because of the complexity of both the nuclear potential and the nuclear many-body problem. It is expected that the preformation factor varies smoothly in the open-shell region [34]. Based on this fact, we take the same preformation factor, $P_\alpha = 0.39$, for all 166 even-even nuclei ranging from $Z = 52$ to $Z = 104$, which means that a single parameter is used for the preformation factor in this model. This is consistent with Buck *et al.*'s model [14] and the value agrees well with both the microscopic calculation for the nucleus ^{210}Po [4] and the experimental results [34].

To gain a better insight into the coupled-channel effect, in Fig. 1 we present the two-channel wave functions in ^{242}Cm, separately corresponding to the $0^+ \to 0^+$ and $0^+ \to 2^+$ channels. As one would expect, in the interior region the $0^+ \to 0^+$ channel function is characterized by 11 nodes while the $0^+ \to 2^+$ channel function is characterized by 10 nodes. This coincides with the Wildermuth and Tang condition [33]. Moreover, the channel functions $u_{n\ell j}(r)$ decrease rapidly outside the nucleus typically by more than 10 orders of magnitude, and in the outer region they have the oscillatory behavior of the irregular Coulomb wave function, with an amplitude decreasing with the distance [24].

As mentioned, the exact treatment of excitation spectrum in the daughter nuclei allows a straightforward calculation of branching ratios. Let us discuss the results of our calculations. We perform the two-channel analysis for well-deformed systems ranging from $Z = 90$ to $Z = 100$. The calculation of branching ratios for α transitions into more highly excited states is similar. Figure 2 shows the comparison of the calculated branching ratios for $0^+ \to 0^+$ α transitions with the experimental ones. Note that information on the branching ratio for $0^+ \to 2^+$ transitions is included by the relationship $b_{2^+} = 100\% - b_{0^+}$. Despite large uncertainties in the measured values of branching ratios, one notices that there is reasonable agreement in both the systematic behavior of the various isotopic chains and the magnitude of branching ratios. So the quantitative description of fine structure in α decay is achieved in our two-channel analysis.

We have performed a systematic calculation of α-decay half-lives within the new version of the GDDCM. The main focus of our investigation is on even-even nuclei ranging from $Z = 52$ to $Z = 104$, consisting of 65 well-deformed α emitters and 101 spherical ones. The exact solution of the full coupled equations (2) is indispensable for well-deformed systems, but in the spherical case it is enough to deal with a single radial equation instead of the full set (2). In our calculations, the only input data are the mass number A and the charge number Z of the parent nucleus, the deformation parameters β_2 and β_4 of the corresponding daughter nucleus [35], and the experimental Q_{J_d} value [36,37]. The calculated α-decay half-lives are found to be in good agreement with the experimental values for all 166 even-even nuclei. Taking the longest-lived nucleus ^{148}Sm with a half-life of 2.21×10^{23} s [38] and the shortest-lived nucleus ^{218}Th with a half-life of 1.09×10^{-7} s [38], for example, our theoretical results for them are, respectively, 4.21×10^{23} and 1.89×10^{-7} s, which are very close to their experimental values.

For the sake of a clear insight into the agreement between experiment and theory, we introduce an agreement factor (AF) into the present analysis that is defined as

$$\text{AF} = 10^{|\log_{10}(T^{\text{cal}}_{1/2}/T^{\text{exp}}_{1/2})|}. \tag{14}$$

For example, the agreement factor AF = 2–3 corresponds to the absolute ratio of theoretical half-lives to experimental ones between 1/3 and 1/2 or between 2 and 3. Figure 3 displays the agreement factor as a function of proton number Z, showing the comparison between calculations and experiments. As one can see, there are 155 decays with AF = 1–3, 8 decays with AF = 3–4, 2 decays with AF = 4–5, and only one decay with AF = 5–6 among all 166 α decays. The largest AF = 5.13 is for the nucleus ^{210}Po. This is consistent with the result of

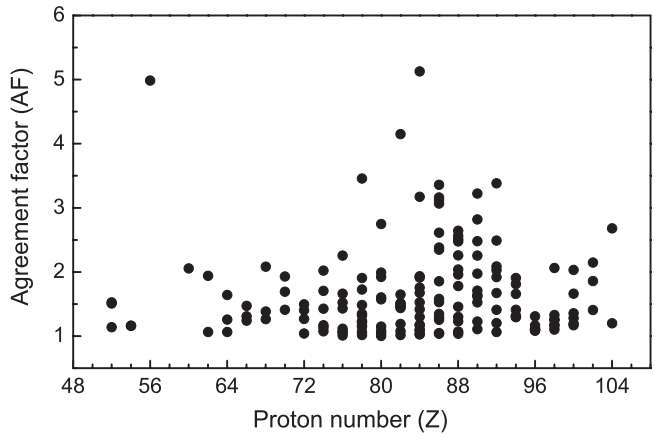

FIG. 3. The agreement factor calculated with the Eq. (14) as a function of proton number Z.

the previous calculations [26]. Such a large deviation can only be explained by the $N = 126$ closed-shell effect, leading to a considerable decrease of the α-preformation factor. Indeed, based on the previous study of exotic α decays around the $N = 126$ shell, we expect that the P_α value in ^{210}Po is 0.062, significantly smaller than the present value 0.39 [20].

To compare the results of the exact formalism presented here with other calculations, we briefly evaluate our overall calculations. In Table I we list the average deviation $\langle\sigma\rangle = \sum_{i=1}^{N} |\log_{10} T^i_{\text{exp.}} - \log_{10} T^i_{\text{cal.}}|/N$ and the root-mean-square (rms) deviation for even-even nuclei. The results obtained using the generalized liquid-drop model (GLDM) [11] and the density-dependent cluster model (DDCM) [26] are also given for comparison. Note that the deviations 0.2, 0.3, and 0.4 of the logarithms correspond to the absolute deviations of half-lives with factors of 1.6, 2.0, and 2.5, respectively. Clearly, all of these models are very successful in calculating α-decay half-lives.

TABLE I. Comparison of the average and rms deviations of the GLDM, the DDCM, and our GDDCM for even-even α emitters. Some new experimental data are taken from Ref. [39].

	GLDM	DDCM	GDDCM
Number	131	157	166
$\langle\sigma\rangle$	–	0.209	0.191
rms	0.35	0.267	0.243

In conclusion, we have presented in this communication a new version of the GDDCM to calculate the decay width. The deformed potential is constructed in the double-folding model by the multipole expansion method. The coupled-channel Schrödinger equation with outgoing wave boundary conditions is used to compute the decay width of well-deformed systems. Exact calculations are performed for 65 well-deformed α emitters and 101 spherical ones. The calculated α-decay half-lives are in excellent agreement with the experimental data, and the experimental branching ratios for well-deformed systems are reproduced. In our approach, the α-preformation factor is taken to be a constant for all the even-even nuclei. In fact, the preformation probability should vary with different parent nuclei, especially for the closed-shell region. In the future, it would be interesting to combine our GDDCM with microscopic calculations of α-preformation amplitudes to achieve a fully microscopic description of the α-decay process.

We are thankful to Chang Xu for helpful discussion and comments. This work is supported by the National Natural Science Foundation of China (Grants 10535010, 10675090, 10775068, 10735010, and 10975072), by the 973 National Major State Basic Research and Development of China (Grant 2007CB815004), by CAS Knowledge Innovation Project No. KJCX2-SW-N02, and by the Research Fund of Doctoral Point (RFDP), No. 20070284016.

[1] G. Gamow, Z. Phys. **51**, 204 (1928).
[2] E. U. Condon and R. W. Gurney, Nature (London) **122**, 439 (1928).
[3] D. S. Delion, A. Sandulescu, and W. Greiner, Phys. Rev. C **69**, 044318 (2004).
[4] K. Varga, R. G. Lovas, and R. J. Liotta, Phys. Rev. Lett. **69**, 37 (1992).
[5] H. F. Zhang and G. Royer, Phys. Rev. C **77**, 054318 (2008).
[6] S. A. Gurvitz and G. Kalbermann, Phys. Rev. Lett. **59**, 262 (1987).
[7] D. N. Poenaru, I. H. Plonski, and W. Greiner, Phys. Rev. C **74**, 014312 (2006).
[8] D. F. Jackson, E. J. Wolstenholme, L. S. Julien, and C. J. Batty, Nucl. Phys. **A316**, 1 (1979).
[9] H. J. Mang, Phys. Rev. **119**, 1069 (1960).
[10] T. L. Stewart, M. W. Kermode, D. J. Beachey, N. Rowley, I. S. Grant, and A. T. Kruppa, Phys. Rev. Lett. **77**, 36 (1996); Nucl. Phys. **A611**, 332 (1996).
[11] G. Royer, J. Phys. G **26**, 1149 (2000).
[12] P. Mohr, Phys. Rev. C **73**, 031301(R) (2006).
[13] J. C. Pei, F. R. Xu, Z. J. Lin, and E. G. Zhao, Phys. Rev. C **76**, 044326 (2007).
[14] B. Buck, A. C. Merchant, and S. M. Perez, Phys. Rev. C **45**, 2247 (1992); At. Data Nucl. Data Tables **54**, 53 (1993).
[15] C. Xu and Z. Ren, Nucl. Phys. **A753**, 174 (2005); **A760**, 303 (2005).
[16] V. Yu. Denisov and H. Ikezoe, Phys. Rev. C **72**, 064613 (2005).
[17] N. G. Kelkar and H. M. Castañeda, Phys. Rev. C **76**, 064605 (2007).
[18] P. Schuurmans *et al.*, Phys. Rev. Lett. **82**, 4787 (1999).
[19] D. S. Delion, S. Peltonen, and J. Suhonen, Phys. Rev. C **73**, 014315 (2006).
[20] D. Ni and Z. Ren, Phys. Rev. C **80**, 014314 (2009).
[21] R. G. Lovas, R. J. Liotta, A. Insolia, K. Varga, and D. S. Delion, Phys. Rep. **294**, 265 (1998).
[22] V. P. Bugrov, S. G. Kadmensky, V. I. Furman, and V. G. Khlebostroev, Sov. J. Nucl. Phys. **41**, 717 (1985).
[23] S. Åberg, P. B. Semmes, and W. Nazarewicz, Phys. Rev. C **56**, 1762 (1997).
[24] D. Ni and Z. Ren, Nucl. Phys. **A825**, 145 (2009).
[25] M. J. Rhoades-Brown *et al.*, Z. Phys. A **310**, 287 (1983).

[26] C. Xu and Z. Ren, Phys. Rev. C **73**, 041301(R) (2006); **74**, 014304 (2006).
[27] S. Peltonen, D. S. Delion, and J. Suhonen, Phys. Rev. C **78**, 034608 (2008).
[28] A. T. Kruppa, B. Barmore, W. Nazarewicz, and T. Vertse, Phys. Rev. Lett. **84**, 4549 (2000); B. Barmore, A. T. Kruppa, W. Nazarewicz, and T. Vertse, Phys. Rev. C **62**, 054315 (2000).
[29] A. M. Kobos, B. A. Brown, P. E. Hodgson, G. R. Satchler, and A. Budzanowski, Nucl. Phys. **A384**, 65 (1982).
[30] G. Bertsch, J. Borysowicz, H. Mcmanus, and W. G. Love, Nucl. Phys. **A284**, 399 (1977).
[31] G. R. Satchler and W. G. Love, Phys. Rep. **55**, 183 (1979).
[32] C. N. Davids and H. Esbensen, Phys. Rev. C **61**, 054302 (2000).
[33] K. Wildermuth and Y. C. Tang, *A Unified Theory of the Nucleus* (Academic Press, New York, 1997).
[34] P. E. Hodgson and E. Běták, Phys. Rep. **374**, 1 (2003).
[35] P. Möller, J. R. Nix, W. D. Myers, and W. J. Swiatecki, At. Data Nucl. Data Tables **59**, 185 (1995).
[36] G. Audi, A. H. Wapstra, and C. Thibault, Nucl. Phys. **A729**, 337 (2003).
[37] R. B. Firestone, V. S. Shirley, C. M. Baglin, S. Y. Frank Chu, and J. Zipkin, *Table of Isotopes*, 8th ed. (Wiley–Interscience, New York, 1996).
[38] G. Audi, O. Bersillon, J. Blachot, and A. H. Wapstra, Nucl. Phys. **A729**, 3 (2003).
[39] NNDC of the Brookhaven National Laboratory, http://www.nndc.bnl.gov.